

# **Validation/Verification of Global Magnetosphere Simulation**

**Aoi Nakamizo (NICT)**

# GEM Workshop (June, 2016)

“Tail Environment and Dynamics at Lunar Distances” FG

“Modeling Methods and Validation” FG

NASA Community Coordinated Modeling Center (CCMC)

Univ. of Michigan  
(SWMF)

FMI  
[Janhunen, 2000]

Lyon-Fedder-Mobarry J. Raeder  
[Lyon et al., 2004]

Table 1. Summary of Features and Settings of Global MHD Models Used in This Study, See the Text for Details

	BATS-R-US	GUMICS-4	LFM	OpenGGCM
MHD equations	ideal, conservative, $B_0 + B_1$	ideal, conservative, $B_0 + B_1$	ideal, semi-conservative, $B_0 + B_1$	semi-conservative with resistivity
Solver notes	eight-wave approximate Riemann	mostly Roe, subcycling, $\nabla \cdot B$ cleaning	total variation diminishing (TVD), constrained transport (CT)	TVD, CT
Order of MHD discretization: spatial / temporal	2 / 2	1 / 1	8 / 2	4 / 2
MHD grid	Cartesian, static, block-refined	Cartesian, dynamic, cell-refined	distorted spherical, static, not refined	stretched Cartesian, static, not refined
Dipole tilt updated with time	yes	no	yes <sup>a</sup>	no
Coordinate system of magnetosphere	GSM	GSE	SM	GSE

<sup>a</sup>The dipole orientation is fixed in SM coordinates, but solar wind and solar EUV conditions are adjusted with time.

# Bursty Bulk Flows in MHD simulation

[Wiltberger et al., 2015]

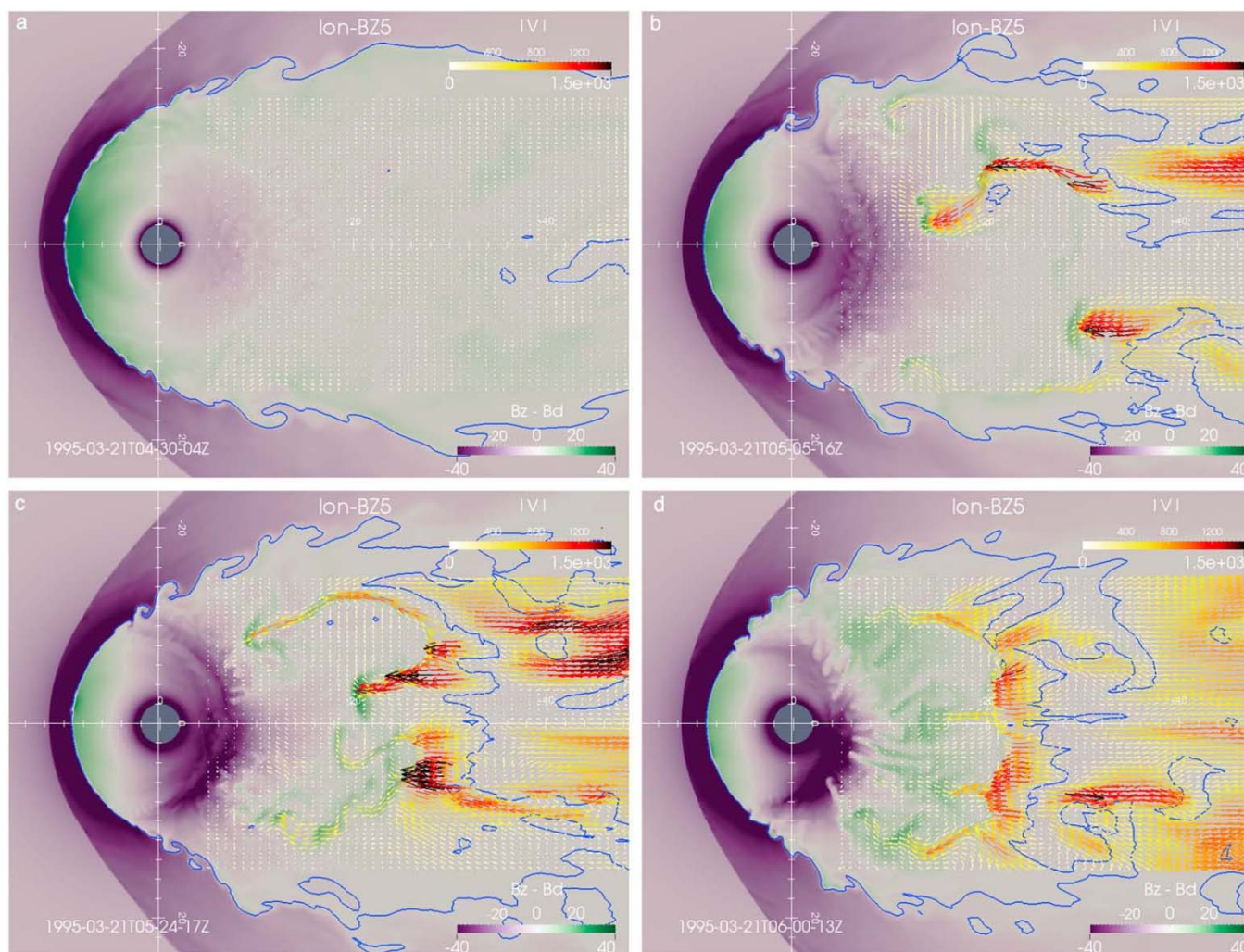


**Figure 1.** Snapshots from the scientific visualization of the magnetotail structure during the simulation interval. In each panel the background cut plane is at  $Z = 0$  and is colored by the difference between the  $B_z$  and the value of dipole field at that location. The colored vector arrows correspond to the 3-D direction of the plasma velocity. Both the length of the vector and the color correspond to the magnitude of the velocity. The blue contour line is drawn at the  $B_z = 0$  value and provides a rough indication of the boundary between open and closed field lines. (a) Simulation at 04:30:04 ST approximately 30 min after the arrival of southward IMF. (b) A single flow channel is clearly seen at 05:05:16 ST, (c) while multiple flow channels are present at 05:24:17 ST. (d) Configuration at the end of the simulation interval 06:00:13 ST.

# Bursty Bulk Flows in MHD simulation

[Wiltberger et al., 2015]

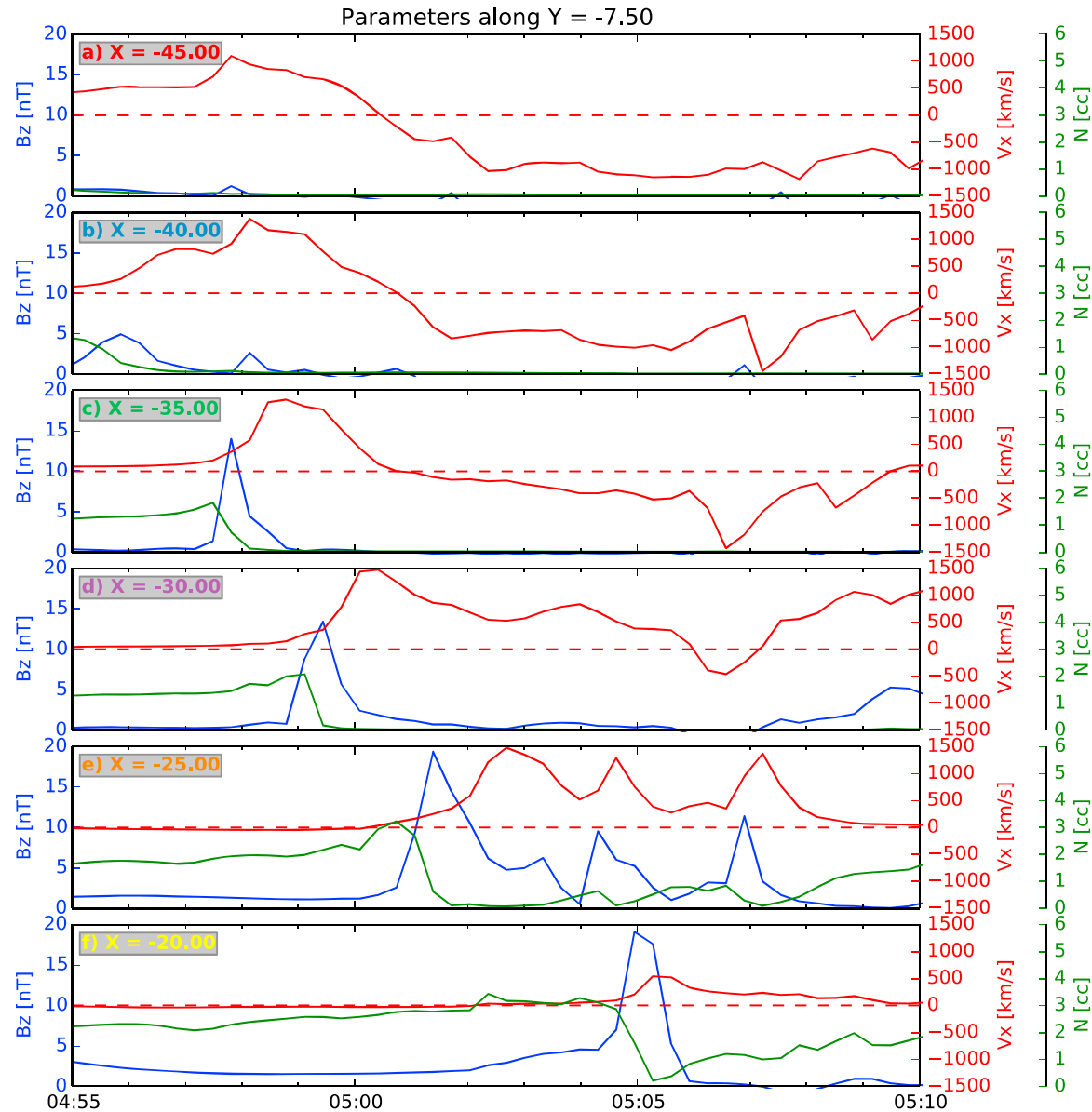


**Figure 3.** Values of density,  $V_x$ , and  $B_z$  at fixed along the path of a BBF. (a–f) Values in  $5 R_E$  steps from  $X = -45$  to  $-20 R_E$ . In each panel density is plotted with the solid green line,  $V_x$  is plotted with a solid red line, and  $B_z$  is plotted with the solid blue line. The color coded on the  $X$  location labeling corresponds to the circle color in Figure 2. The plot covers 15 min during which time the BBF covers the entire range of  $X$  values shown in the plot.

# Bursty Bulk Flows in MHD simulation

[Wiltberger et al., 2015]

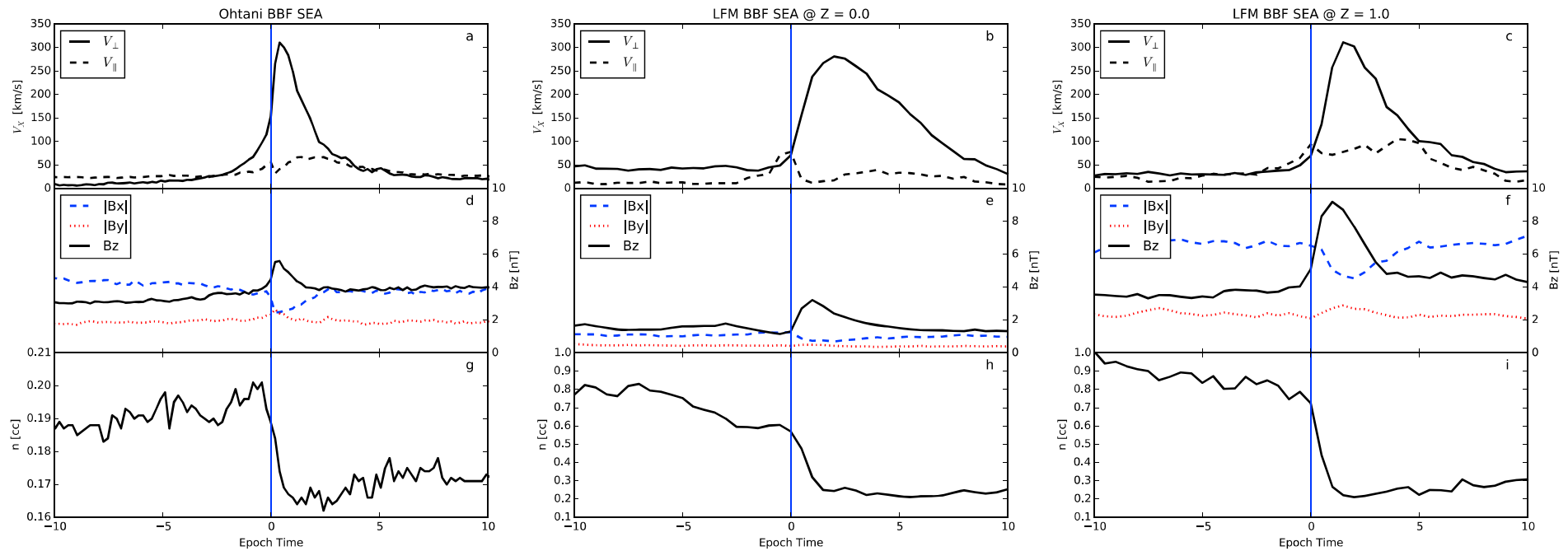


**Figure 5.** Comparison of the Ohtani2004 superposed epoch analysis of Geotail BBF data with results from a superposed epoch analysis using the same selection criteria constructed from the high-resolution LFM simulations. (a, d, and g) Data taken from Figure 3 of Ohtani2004. (b, e, and h) Data from the LFM simulation at the  $Z = 0.0$  plane. (c, f, and i) Data from the  $Z = 1.0$  plane of the simulation. Figures 5a–5c show the  $V_{\perp X}$  and  $V_{\parallel}$  comparisons. Figures 5d–5f compare the magnetic field properties between the data and observations. Figures 5g–5i compare the density changes. Note that in this last row unlike the previous rows, the Geotail and LFM results are presented using different y scales.

# Global Magnetosphere Simulation

## Ideal MHD Equation System

$$\frac{\partial}{\partial t}(\rho) + \nabla \cdot (\rho \mathbf{V}) = 0,$$

$$\frac{\partial}{\partial t}(\rho \mathbf{V}) + \nabla \cdot \left( \rho \mathbf{v} \mathbf{v} + p \mathbf{I} + \frac{B^2 - B_0^2}{2\mu_0} \mathbf{I} - \frac{\mathbf{B} \mathbf{B} - \mathbf{B}_0 \mathbf{B}_0}{2\mu_0} \right) = 0,$$

$$\frac{\partial}{\partial t}(U_1) = \nabla \cdot \left[ \mathbf{v} \cdot \left( U_1 + p + \frac{B_1^2}{2\mu_0} \right) - \frac{\mathbf{B}_1(\mathbf{v} \cdot \mathbf{B}_1)}{\mu_0} - \frac{\mathbf{B}_0(\mathbf{v} \cdot \mathbf{B}_1)}{\mu_0} + \frac{\mathbf{v}(\mathbf{B}_1 \cdot \mathbf{B}_0)}{\mu_0} \right] = 0,$$

$$\frac{\partial}{\partial t} \mathbf{B}_1 + \nabla \times (\mathbf{v} \times \mathbf{B}) = 0,$$

$$U_1 = \frac{\rho V^2}{2} + \frac{p}{\gamma - 1} + \frac{B_1^2}{2\mu_0},$$

$$\mathbf{B} = \mathbf{B}_0 + \mathbf{B}_1,$$

$$\mathbf{E} = -\mathbf{v} \times \mathbf{B}$$



## Generalized Ohm's Law

$$\mathbf{E} = -\mathbf{v} \times \mathbf{B} + \frac{1}{n_e} \mathbf{J} \times \mathbf{B} - \frac{1}{ne} \nabla \cdot p_e + \eta \mathbf{J} + \frac{m_e}{e^2 n} \left[ \frac{\partial \mathbf{J}}{\partial t} + \nabla \cdot (\mathbf{J} \mathbf{V} + \mathbf{V} \mathbf{J}) \right]$$

(742,621)

$\mathbf{J}_{\parallel} (\sim \nabla \times \mathbf{B})$

input

$\mathbf{V}_{\perp} (= -(\nabla \Phi) \times \mathbf{B})$

update

Iono